

The first dinosaur egg was soft

<https://doi.org/10.1038/s41586-020-2412-8>

Received: 19 March 2019

Accepted: 14 May 2020

Published online: 17 June 2020

 Check for updates

Mark A. Norell¹✉, Jasmina Wiemann²✉, Matteo Fabbri²✉, Congyu Yu¹, Claudia A. Marsicano³, Anita Moore-Nall⁴, David J. Varricchio⁴, Diego Pol⁵ & Darla K. Zelenitsky⁶

Calcified eggshells protect developing embryos against environmental stress and contribute to reproductive success¹. As modern crocodylians and birds lay hard-shelled eggs, this eggshell type has been inferred for non-avian dinosaurs. Known dinosaur eggshells are characterized by an innermost membrane, an overlying protein matrix containing calcite, and an outermost waxy cuticle^{2–7}. The calcitic eggshell consists of one or more ultrastructural layers that differ markedly among the three major dinosaur clades, as do the configurations of respiratory pores. So far, only hadrosaurid, a few sauropodomorph and tetanuran eggshells have been discovered; the paucity of the fossil record and the lack of intermediate eggshell types challenge efforts to homologize eggshell structures across all dinosaurs^{8–18}. Here we present mineralogical, organochemical and ultrastructural evidence for an originally non-biomineralized, soft-shelled nature of exceptionally preserved ornithischian *Protoceratops* and basal sauropodomorph *Mussaurus* eggs. Statistical evaluation of in situ Raman spectra obtained for a representative set of hard- and soft-shelled, fossil and extant diapsid eggshells clusters the originally organic but secondarily phosphatized *Protoceratops* and the organic *Mussaurus* eggshells with soft, non-biomineralized eggshells. Histology corroborates the organic composition of these soft-shelled dinosaur eggs, revealing a stratified arrangement resembling turtle soft eggshell. Through an ancestral-state reconstruction of composition and ultrastructure, we compare eggshells from *Protoceratops* and *Mussaurus* with those from other diapsids, revealing that the first dinosaur egg was soft-shelled. The calcified, hard-shelled dinosaur egg evolved independently at least three times throughout the Mesozoic era, explaining the bias towards eggshells of derived dinosaurs in the fossil record.

Hard-shelled eggs are an important character defining modern birds and are thought to have had a key role in their survival through the Cretaceous–Palaeogene extinction (approximately 66 million years ago)¹. The calcified avian eggshell stands in contrast to the primitive amniote eggshell condition: early amniotes and more primitive tetrapods^{2–7} laid soft eggshells. Extant archosaurs share assembly-line oviducts⁸, corpus luteum morphology⁹ and the embryonic resorption of eggshell calcite—factors that would seem to suggest homology of hard, calcitic eggshell among crocodylians and all dinosaurs, non-avian and avian^{10–14}. However, pterosaurs—the sister group to dinosauriforms—laid soft eggs^{15–18}.

Non-avian dinosaurs are thought to have shared with crocodylians, extant birds and most turtles an innermost shell membrane⁶, a biomineralized protein matrix and an outer cuticle⁶. Such architecture is found in most previously described dinosaur eggs, regardless of shape, size or colour¹⁹. Both the shell membrane and the biomineralized protein matrix are arranged in multiple layers of varying internal patterning. Calcitic dinosaur eggs²⁰ are generally considered hard tissues, and their fossil record is patchy in terms of diversity and age²¹. Only eggs of a few taxa—such as ornithopods, sauropodomorphs,

titanosaurs and tetanurans—have been reliably identified^{21–26}. The vast majority of these eggs are from the Cretaceous period^{21–28}. However, the diversity of dinosaur taxa from the Triassic period to the Cretaceous suggests that the apparent biases in the egg fossil record cannot be explained solely by preferential preservation of certain nesting sites, as previously hypothesized. Even in highly fossiliferous localities, such as the Mongolian Djadokhta^{26–29} and the Tugrugeen Shireh site³⁰, where eggs and embryonic remains are relatively common, eggshells attributable to more basal dinosaur taxa have not been recovered.

Previous attempts to homologize archosaur eggshell ultrastructures failed^{24,29} because of fundamental differences in the layer organization^{23–29,31}. Ornithopod eggshells^{23–25,29} have one calcified spherulitic layer. Basal sauropodomorph eggshell^{32–35} consists primarily of a thick membrane covered by a thin, nondescript calcitic layer^{32–35}, and titanosaurid sauropod eggshells^{22,36} possess a single, well-calcified spherulitic layer on a thinner membrane^{22,36,37}. The number of calcified ultrastructural layers in theropod eggshells varies between one and three^{22–24,26–29,31,38,39}. Current hypotheses assume a single evolutionary origin of the dinosaurian calcified egg^{11–13}.

¹Division of Vertebrate Paleontology, American Museum of Natural History, New York, NY, USA. ²Department of Geology & Geophysics, Yale University, New Haven, CT, USA. ³Departamento de Ciencias Geológicas, Universidad de Buenos Aires, Buenos Aires, Argentina. ⁴Department of Earth Sciences, Montana State University, Bozeman, MT, USA. ⁵CONICET, Museo Paleontológico Egidio Feruglio, Trelew, Argentina. ⁶Department of Geoscience, University of Calgary, Calgary, Alberta, Canada. ✉e-mail: norell@amnh.org; jasmina.wiemann@yale.edu; matteo.fabbri@yale.edu

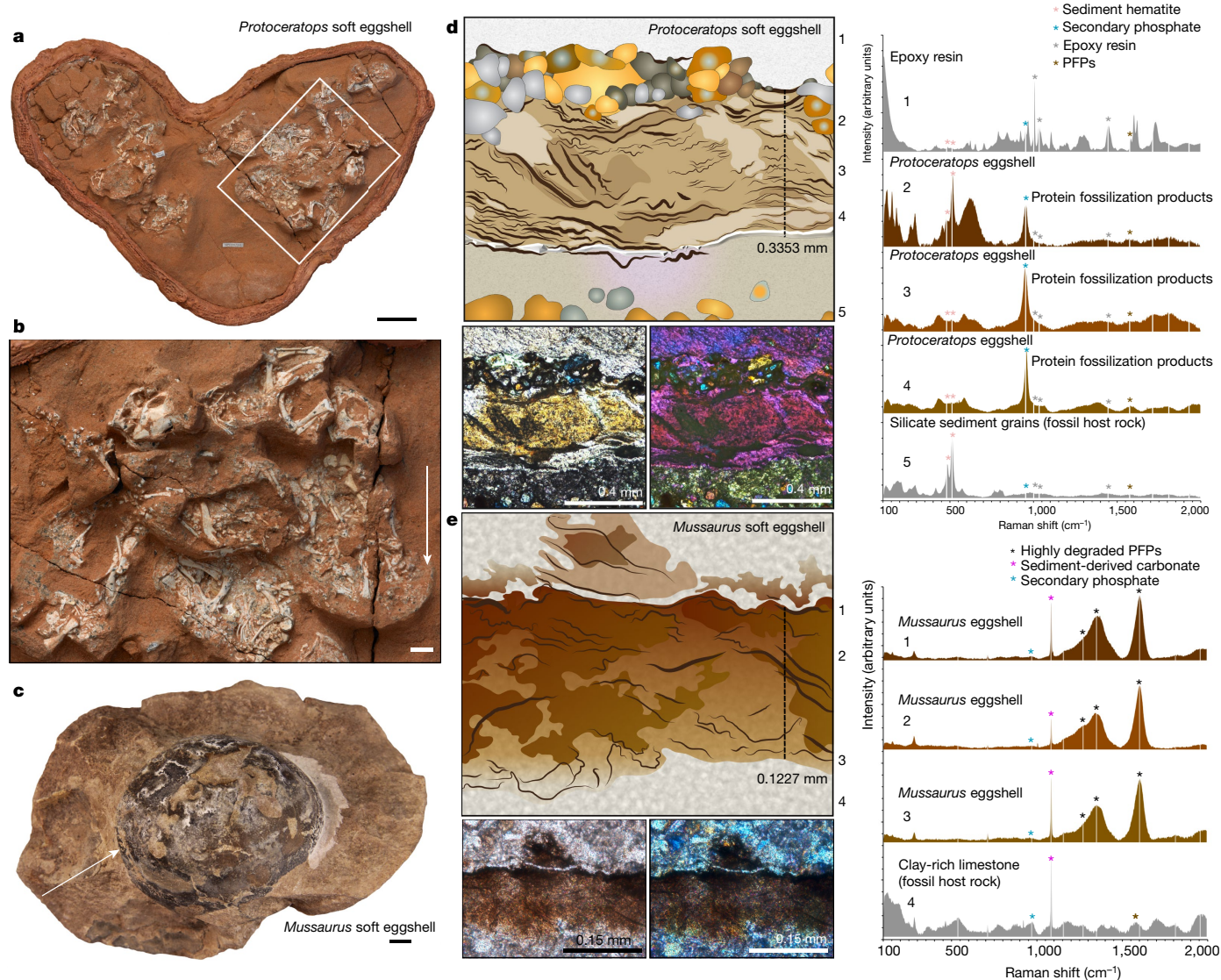


Fig. 1 | Photographs, histology and Raman spectroscopy of *Protoceratops* and *Mussaurus* soft eggshells. **a, b**, Clutch assigned to the basal ceratopsian *Protoceratops* (**a**) on the basis of embryonic remains (**b**). The white outlined area in **a** corresponds to **b**; the arrow in **b** indicates one of the white, egg-shaped halos surrounding the embryos. **c**, Egg assigned to the basal sauropodomorph *Mussaurus*. The arrow indicates the black egg-shaped halo. Scale bars, 50 mm (**a**), 10 mm (**b, c**). **d**, Schematic (top) of the microstructures observed in a representative *Protoceratops* section (bottom; one of six technical replicates), depicted in normal (bottom left) and cross-polarized (bottom right) light. The eggshell is multilayered and dark brown; birefringence is observed. The

maximum eggshell thickness measures 0.3053 mm (0.3353 mm including the phosphatized layer). Raman point spectra (right) were acquired at the positions labelled with bold numbers, each spectrum with ten technical replicates, at three distinct eggshell positions (the same applies to **e**). PFPs are in brown, and epoxy and sediment are in grey. **e**, Schematic (top) of microstructures in the *Mussaurus* section (bottom) under normal (bottom left) and cross-polarized (bottom right) light. Multiple layers are evident within the eggshell, which lacks birefringence. The maximum eggshell thickness measures 0.1227 mm.

Here we challenge this idea of a single evolutionary origin of hard-shelled dinosaur eggs by analysing embryo-bearing, soft-shelled ceratopsian and basal sauropodomorph eggshells, and reveal through new organochemical, ultrastructural and statistical analyses that hard-shelled eggs evolved at least three times independently in dinosaurs.

We analysed an exceptionally preserved ornithischian egg clutch (IGM 100/1021), attributed to *Protoceratops*, from the Ukhaa Tolgod locality (Campanian/Upper Cretaceous) in Mongolia^{1,2}. This specimen comprises a clutch of at least 12 eggs and embryos (Fig. 1a, b), 6 of which preserve nearly complete skeletons (Fig. 1b). Although all vertebral elements remain unfused, the pedal phalanges including unguals are ossified. Nine of the 12 embryos preserve long bone elements, which differ in size by at most 15%, indicating individuals of comparable developmental stage.

Associated with most of these embryos is a diffuse black and white egg-shaped halo (Fig. 1b). This halo surrounds various individuals, obscuring some skeletal elements. Most of the embryo vertebral columns and limbs are flexed, consistent with *in ovo* preservation. Combined outlines of eggs and embryos suggest an ellipsoidal egg of approximately 121–125 mm by 60 mm. By contrast, two potentially hatched neonates rest dorsal side down with their vertebral column fully extended and limbs oriented out to the sides. These two individuals are largely free of the mineral halos that surround the remaining late-stage embryos.

Histological evaluation of the egg-shaped halos reveals a 305.3- μm -thick (maximum thickness), dark brown, semi-transparent and multilayered (Fig. 1d, e and Supplementary Fig. 1) carbonaceous zone on top of a 30- μm -thick (maximum), white crystalline layer. The

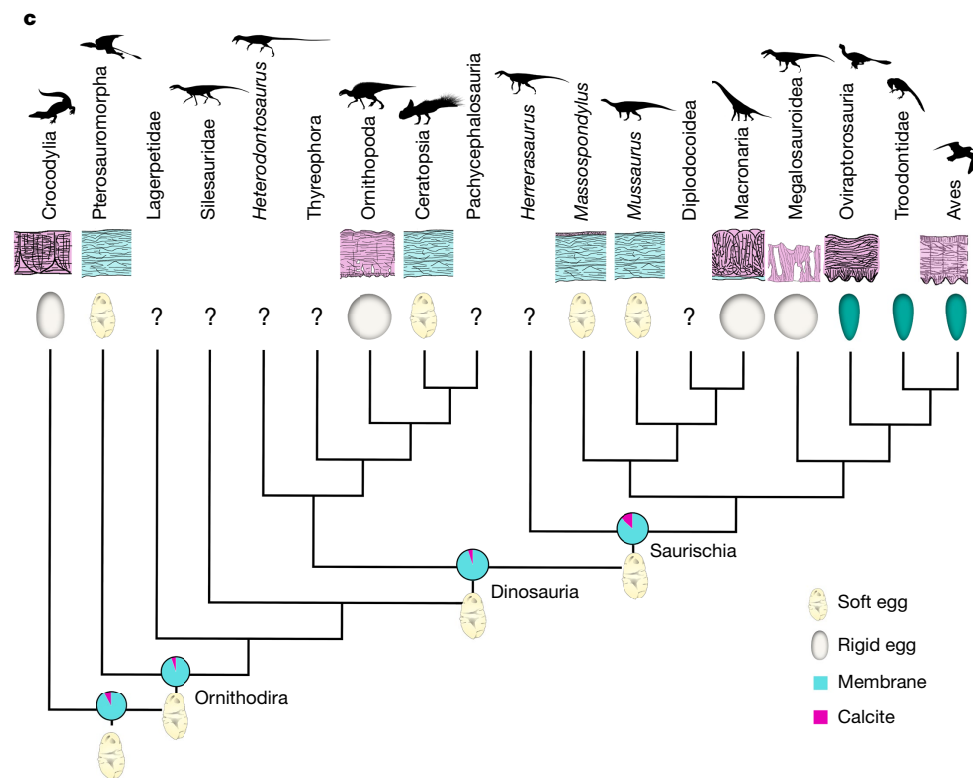
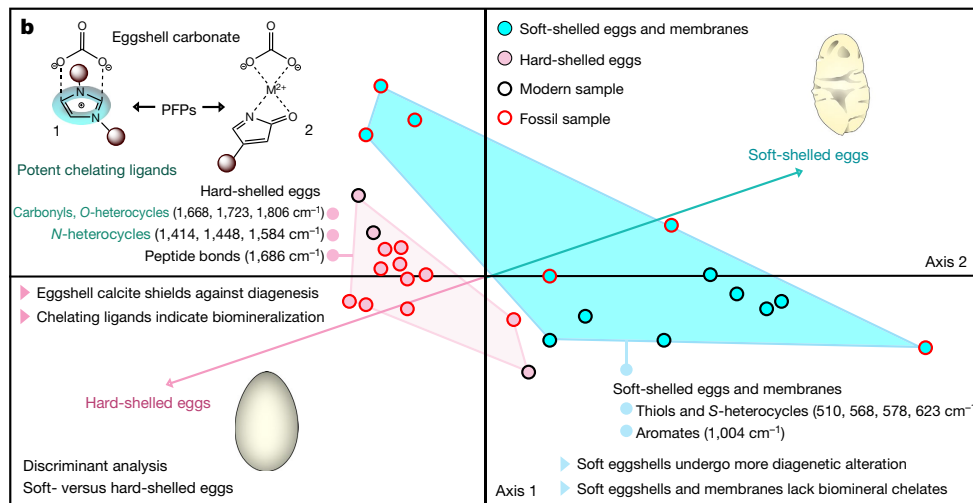
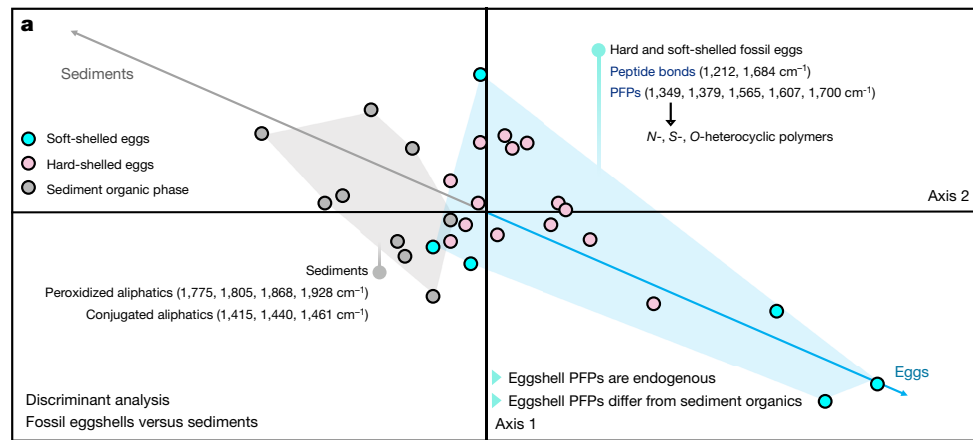


Fig. 2 | Biomineralization and evolution of hard- and soft-shelled eggs. **a**, Discriminant analysis of informative Raman bands ($n = 14$) in fossil eggshells ($n = 20$) and sediments ($n = 9$). The blue (eggs) and grey (sediment) vectors characterize how the sample groups diverge. **b**, Discriminant analysis of Raman bands ($n = 12$; spectra acquired with 10 technical replicates) of proteins (and PFPs) in soft-shelled ($n = 13$) and hard-shelled ($n = 13$) fossil and extant eggs. Turquoise and pink dots indicate soft-shelled and hard-shelled eggs, respectively, and the corresponding vectors characterize how samples diverge. Discriminant factors are listed for each cluster. Chelating ligands are present only in biomineralized eggshells, and are absent in soft eggs. **c**, Simplified phylogeny showing the evolution of eggshell in Archosauria ($n = 18$ taxa shown, based on $n = 112$ diapsid taxa). Mechanically soft eggshell is found to be ancestral for Archosauria, Ornithodira and Dinosauria. The schematics of eggshell structures distinguish membrane (blue) and crystalline (pink) layers. Coloured eggs mark the appearance of egg colour¹⁹.

absence of birefringence or extinction in the brown eggshell layer, as well as its irregular arrangement in cross-section and its apparently pliable nature even when fossilized, suggests an organic composition (Fig. 1d). In situ Raman spectroscopy corroborates an organic composition of the brown eggshell layer, and reveals the presence of protein fossilization products^{40,41} (PFPs) and phosphate (the white layer) in the *Protoceratops* eggshell. Neither phosphate nor comparable PFPs are found in the associated sediment. PFPs in the *Protoceratops* eggshells contain relatively high amounts of S-heterocycles, which are characteristic of eggshell-derived organic matter^{19,40,41}.

Our sample also includes eggs attributed to the basal sauropodomorph *Mussaurus* (Fig. 1c) from the Laguna Colorado Formation (Late Triassic/Early Jurassic). These eggs were found at the same locality and stratigraphic level as the type material of *Mussaurus patagonicus*⁴². Several eggs preserve embryonic and juvenile specimens, and preserved mandibles bear apomorphic features of *M. patagonicus*⁴³. The thin eggshell stands out from the grey-whitish micritic limestone sediment owing to its dark-brown colour. Histological evaluation reveals a 122.7- μm -thick (maximum thickness), dark brown, semi-transparent, apparently multilayered carbonaceous film (Fig. 1d, e and Supplementary Fig. 1), comparable to the *Protoceratops* soft eggshell. The dark brown layer shows no birefringence under cross-polarized light, consistent with an organic composition (Fig. 1e). In situ Raman spectroscopic assessment identifies peroxidized PFPs in the eggshell organic layers^{19,40,41} (Fig. 1e; see Supplementary Table 2 for band assignments). A calcite signal associated with the *Mussaurus* eggshell is identical in crystallinity and Raman shift to the surrounding limestone sediment (Fig. 1e), and given that we identified no eggshell minerals through polarized light microscopy (Fig. 1e), we attribute this signal to sedimentary calcite (Supplementary Fig. 2).

We used Raman spectroscopy to fingerprint the chemical composition of *Protoceratops*, *Mussaurus* and other extant and extinct diapsid eggshells ($n = 26$), as well as associated sediment samples ($n = 9$) (Supplementary Table 2). For each sample, we extracted relative intensities at $n = 12$ Raman band signals characterizing the organic phase in fossil eggshells and sediments (Fig. 2a and Supplementary Table 1). In addition, for all eggshell samples we compiled relative intensities of $n = 14$ Raman bands characteristic of proteins (extant samples) and PFPs (fossil samples) (Fig. 2b), and converted the intensities to a taxon-character matrix. We used the dataset on the eggshell and sediment organic phase in a discriminant analysis, and used the protein/PFP dataset to discriminate biomineralized and non-biomineralized components in both fossil and extant eggshells.

The eggshell-sediment discriminant analysis revealed that the key compositional difference between fossil eggshells and sediments is the presence of increased quantities of PFPs (*N*-, *O*- and *S*-heterocycles) and unaltered peptide bonds in the hard- and soft-shelled eggs (Fig. 2a). The peptide bonds and abundant PFPs in fossil eggshells are therefore identified as endogenous, whereas sediment organics are mostly peroxidized aliphatics⁴¹ (Fig. 2a).

Analysing the protein/PFP data for fossil and extant soft (non-biomineralized) and hard (biomineralized) eggs revealed that non-biomineralized eggshell proteins/PFPs are characteristically enriched in thiols, thioethers and *S*-heterocycles and appear rather degraded⁴¹ (Fig. 2a). Hard eggshells preserve PFPs with still-intact peptide bonds and contain abundant chelating ligands—that is, organic groups that engage with the mineral phase⁴¹. We identify carbonyls, *N*-heterocycles and *O*-heterocycles as potent mineral-coordinating ligands in eggshell proteins (extant samples) and PFPs (fossil samples); they represent suitable markers for assessing biomineralization in fossils⁴¹.

Hierarchical clustering of selected protein/PFP Raman bands from 24 diapsid samples grouped *Protoceratops* and *Mussaurus* eggshells with non-biomineralized, soft eggs separately from a cluster of biomineralized, hard eggs (Extended Data Fig. 1; see details in Supplementary

Information, section 2). We included extracted shell membranes from modern eggshells to prevent phylogenetic attraction of proteins/PFPs in the cluster analysis⁴¹ (Supplementary Information, section 2). The extracted eggshell membranes clustered with soft eggshells as non-biomineralized proteins/PFPs.

Using these biomineralization data and available eggshell mechanical properties in the literature (Methods and Supplementary Information sections 2, 7), we ran an ancestral-state reconstruction with both parsimony and likelihood algorithms to elucidate the nature of the eggshell at the divergence of the three major clades of dinosaurs (Fig. 2c, Supplementary Figs. 3–8 and Supplementary Tables 3, 4). We found that the first dinosaur egg was soft-shelled and that rigid, calcified eggshell evolved independently in the three major lineages of dinosaurs. This convergent acquisition of eggshell calcification in dinosaurs is paralleled by that in other reptiles^{6,7} and resolves previous problems in homologizing ultrastructural layers in dinosaur eggs³⁷: the calcitic eggshells of ornithopods, sauropods and theropods are not homologous. These independent origins explain the increased number of eggshells found at different localities towards the Late Cretaceous as advanced ornithopods, titanosaurs and tetanurans diversified²⁷.

Mussaurus and *Protoceratops* laid, as with many other dinosaurs, soft eggs that placed entirely different demands on the nesting environment. Soft eggshells are more sensitive to water loss (and therefore cannot be stored in the open⁶), and offer little protection against mechanical stressors, such as a brooding parent. Dinosaurs laying soft-shelled eggs probably buried them in moist sand or soil, where the developing embryos relied on external incubation (such as heat resulting from decomposing vegetation) and parental nest care included, at most, nest guarding.

In conclusion, the non-biomineralized, soft nature of both *Protoceratops* and *Mussaurus* eggs provides direct evidence for the independent evolution of calcified eggs in dinosaurs. This discovery ties in with recent findings of several reproductive traits, such as egg colour^{19,44}, paternal nest care^{19,20,23} and open nest structures^{19,20}, that are confined to theropod dinosaurs, representing an independent lineage of eggshell evolution. The reproductive physiology of theropods differs considerably from that of derived ornithischians and sauropods, and may have played a key part in the Cretaceous–Palaeogene survival and radiation of modern birds.

Online content

Any methods, additional references, Nature Research reporting summaries, source data, extended data, supplementary information, acknowledgements, peer review information; details of author contributions and competing interests; and statements of data and code availability are available at <https://doi.org/10.1038/s41586-020-2412-8>.

- Erickson, G. M., Zelenitsky, D. K., Kay, D. I. & Norell, M. A. Dinosaur incubation periods directly determined from growth-line counts in embryonic teeth show reptilian-grade development. *Proc. Natl Acad. Sci. USA* **114**, 540–545 (2017).
- Romer, A. S. Origin of the amniote egg. *Sci. Monthly* **85**, 57–63 (1957).
- Sander, P. M. Reproduction in early amniotes. *Science* **337**, 806–808 (2012).
- Hadek, R. The structure of the mammalian egg. *Int. Rev. Cytol.* **18**, 29–71 (1965).
- Hou, L. H., Li, P. P., Ksepka, D. T., Gao, K. Q. & Norell, M. A. Implications of flexible-shelled eggs in a Cretaceous choristoderan reptile. *Proc. R. Soc. B* **277**, 1235–1239 (2010).
- Packard, M. J., Packard, G. C. & Boardman, T. J. Structure of eggshells and water relations of reptilian eggs. *Herpetologica* **38**, 136–155 (1982).
- Schleich, H. H. & Kästle, W. *Reptile Egg-Shells* (Gustav Fischer, 1988).
- Palmer, B. D. & Guillette, L. J. Jr. Alligators provide evidence for the evolution of an archosaurian mode of oviparity. *Biol. Reprod.* **46**, 39–47 (1992).
- Coombs, W. P. Modern analogs for dinosaur nesting and parental behavior. *Geol. Soc. Am.* **238**, 21–54 (1989).
- Varricchio, D. J., Jackson, F. & Trueman, C. N. A nesting trace with eggs for the Cretaceous theropod dinosaur *Troodon formosus*. *J. Vertebr. Paleontol.* **19**, 91–100 (1999).
- Mikhailov, K. E. *Fossil and Recent Eggshell in Amniotic Vertebrates: Fine Structure, Comparative Morphology and Classification* (Special Papers in Palaeontology No. 56) (1997).
- Isles, T. E. The socio-sexual behaviour of extant archosaurs: implications for understanding dinosaur behaviour. *Hist. Biol.* **21**, 139–214 (2009).

13. Piñero, G., Ferigolo, J., Meneghel, M. & Laurin, M. The oldest known amniotic embryos suggest viviparity in mesosaurs. *Hist. Biol.* **24**, 620–630 (2012).
14. Ji, Q. et al. Pterosaur egg with a leathery shell. *Nature* **432**, 572 (2004).
15. Wang, X. et al. Egg accumulation with 3D embryos provides insight into the life history of a pterosaur. *Science* **358**, 1197–1201 (2017).
16. Chiappe, L. M., Codorniu, L., Grellet-Tinner, G. & Rivaola, D. Argentinian unhatched pterosaur fossil. *Nature* **432**, 571–572 (2004).
17. Lü, J. et al. An egg-adult association, gender, and reproduction in pterosaurs. *Science* **331**, 321–324 (2011).
18. Unwin, D. M. & Deeming, D. C. Pterosaur eggshell structure and its implications for pterosaur reproductive biology. *Zitteliana* **28**, 199–207 (2008).
19. Wiemann, J., Yang, T. R. & Norell, M. A. Dinosaur egg colour had a single evolutionary origin. *Nature* **563**, 555–558 (2018).
20. Yang, T. R., Chen, Y. H., Wiemann, J., Spiering, B. & Sander, P. M. Fossil eggshell cuticle elucidates dinosaur nesting ecology. *PeerJ* **6**, e5144 (2018).
21. Araújo, R. et al. Filling the gaps of dinosaur eggshell phylogeny: Late Jurassic Theropod clutch with embryos from Portugal. *Sci. Rep.* **3**, 1924 (2013).
22. Chiappe, L. M. et al. Sauropod dinosaur embryos from the Late Cretaceous of Patagonia. *Nature* **396**, 258–261 (1998).
23. Varricchio, D. J. & Jackson, F. D. Reproduction in Mesozoic birds and evolution of the modern avian reproductive mode. *Auk* **133**, 654–684 (2016).
24. Grellet-Tinner, G., Chiappe, L. M., Norell, M. & Bottjer, D. Dinosaur eggs and nesting behaviors: a paleobiological investigation. *Palaeogeogr. Palaeoclimatol. Palaeoecol.* **232**, 294–321 (2006).
25. Horner, J. R. Evidence of colonial nesting and 'site fidelity' among ornithischian dinosaurs. *Nature* **297**, 675–676 (1982).
26. Carpenter, K. *Eggs, Nests, and Dinosaur Babies: A Look At Dinosaur Reproduction* (Indiana Univ. Press, 1999).
27. Norell, M. A. et al. A theropod dinosaur embryo and the affinities of the flaming cliffs dinosaur eggs. *Science* **266**, 779–782 (1994).
28. Norell, M. A., Clark, J. M., Chiappe, L. M. & Dashzeveg, D. A nesting dinosaur. *Nature* **378**, 774–776 (1995); erratum 379, 186 (1996).
29. Mikhailov, K. E. Eggshell structure, parataxonomy and phylogenetic analysis: some notes on articles published from 2002 to 2011. *Hist. Biol.* **26**, 144–154 (2014).
30. Kielan-Jaworowska, Z. & Dashzeveg, D. New Late Cretaceous mammal locality in Mongolia and a description of a new multituberculate. *Acta Palaeontol. Pol.* **23**, 115–130 (1978).
31. Zelenitsky, D. K. & Therrien, F. Phylogenetic analysis of reproductive traits of maniraptoran theropods and its implications for egg parataxonomy. *Palaeont.* **51**, 807–816 (2008).
32. Zelenitsky, D. K. & Modesto, S. P. Re-evaluation of the eggshell structure of eggs containing dinosaur embryos from the Lower Jurassic of South Africa. *S. Afr. J. Sci.* **98**, 407–408 (2002).
33. Reisz, R. R., Scott, D., Sues, H. D., Evans, D. C. & Raath, M. A. Embryos of an early Jurassic prosauropod dinosaur and their evolutionary significance. *Science* **309**, 761–764 (2005).
34. Stein, K. et al. Structure and evolutionary implications of the earliest (Sinemurian, Early Jurassic) dinosaur eggs and eggshells. *Sci. Rep.* **9**, 4424 (2019).
35. Reisz, R. R. et al. Embryology of Early Jurassic dinosaur from China with evidence of preserved organic remains. *Nature* **496**, 210–214 (2013).
36. Wilson, J. A., Mohabey, D. M., Peters, S. E. & Head, J. J. Predation upon hatchling dinosaurs by a new snake from the late Cretaceous of India. *PLoS Biol.* **8**, e1000322 (2010).
37. Mikhailov, K. E. Classification of fossil eggshells of amniotic vertebrates. *Acta Pal. Pol.* **36**, 193–238 (1991).
38. Varricchio, D. J., Jackson, F., Borkowski, J. J. & Horner, J. R. Nest and egg clutches of the dinosaur *Troodon formosus* and the evolution of avian reproductive traits. *Nature* **385**, 247–250 (1997).
39. Kundrát, M., Cruickshank, A. R. I., Manning, T. W. & Nudds, J. Embryos of therizinosaurid theropods from the Upper Cretaceous of China: diagnosis and analysis of ossification patterns. *Acta Zool.* **89**, 231–251 (2008).
40. Wiemann, J. et al. Fossilization transforms vertebrate hard tissue proteins into N-heterocyclic polymers. *Nat. Commun.* **9**, 4741 (2018).
41. Wiemann, J., Crawford, J. M. & Briggs, D. E. G. Phylogenetic and physiological signals in metazoan fossil biomolecules. *Sci. Adv.* (in press).
42. Bonaparte, J. F. & Martin, V. El hallazgo del primer nido de dinosaurios Triásicos, (Saurischia, Prosauropoda), Triásico superior de Patagonia, Argentina. *Ameghiniana* **16**, 173–182 (1979).
43. Pol, D. & Powell, J. E. Skull anatomy of *Mussaurus patagonicus* (Dinosauria: Sauropodomorpha) from the late Triassic of Patagonia. *Hist. Biol.* **19**, 125–144 (2007).
44. Wiemann, J., Yang, T. R. & Norell, M. A. Reply to: Egg pigmentation probably has an Archosaurian origin. *Nature* **570**, E46–E50 (2019).

Publisher's note Springer Nature remains neutral with regard to jurisdictional claims in published maps and institutional affiliations.

© The Author(s), under exclusive licence to Springer Nature Limited 2020

Methods

Small fragments of egg-shaped halos and surrounding sediments in the *Protoceratops* (IGM 100/1021) and *Mussaurus* samples were thin-sectioned, photographed and redrawn. Eggshells of extant taxa (Supplementary Table 2) were decalcified in 2 M hydrochloric acid, rinsed in deionized water, and dried onto microscope glass slides. Raman microspectroscopy was performed on modern and fossil eggshells and membranes ($n = 26$ eggshells and $n = 9$ sediments), using a Horiba LabRam HR800 (Department of Geology and Geophysics, Yale University, CT) with 532 nm excitation (20 mW, 20 s, 10 technical replicates). The spectra were obtained over the range from 100–2,000 cm^{-1} and processed in LabSpec 5 (Supplementary Information, section 2). Intensities in eggshell and sediment spectra were selected for two band sets (Supplementary Tables 1, 2): a dataset covering signals of organics in both eggshells and sediments, and a dataset covering eggshell protein and PFPs (listed in Fig. 2a, b). These datasets (Fig. 2a, b) were converted into variance–covariance matrices, and subjected to discriminant analyses in PAST 3.0.

On the basis of the eggshell data and the published literature, we carried out both parsimony- and likelihood-based ancestral-state reconstructions ($n = 112$ extinct and extant diapsid taxa). As the published literature did not assess biomineralization, but rather mechanical eggshell properties, coding distinguished between soft, semi-rigid and rigid eggshells on the basis of the relative thickness of eggshell membrane and crystalline layer (soft, less than 50%; semi-rigid, 50–67%; rigid, more than 67%). Sample randomization and blinding do not apply to this study (see Supplementary Information, section 2 for details).

Reporting summary

Further information on research design is available in the Nature Research Reporting Summary linked to this paper.

Data availability

All relevant Raman spectra and eggshell codings are available within this paper and its Supplementary Information. Materials are available from the corresponding authors upon reasonable request.

Acknowledgements We thank M. Ellison for the *Protoceratops* clutch photography; G. Watkins-Colwell and K. Zyskowski for providing eggshell specimens from the Yale Peabody collections; and D. E. G. Briggs for comments on the manuscript. J. Headden, S. Hartman, E. Willoughby and M. Witton created the PhyloPic silhouettes used in Fig. 2. A grant to D.P. from the National Geographic Society (grant 8860-10) funded the collection of *Mussaurus* eggshells.

Author contributions M.A.N. designed the project. M.A.N., J.W. and M.F. conceived and designed the experiments. M.A.N., C.Y., C.A.M., D.J.V., D.P. and D.K.Z. contributed material and/or material information. J.W., D.J.V. and A.M.-N. prepared thin sections. J.W. designed the Raman protocol, performed Raman spectroscopy, developed the proxies and analysed the data. M.F. described the clutches, coded eggshells and performed the ancestral-state reconstruction. M.A.N., J.W. and M.F. wrote the manuscript with input from all authors.

Competing interests The authors declare no competing interests.

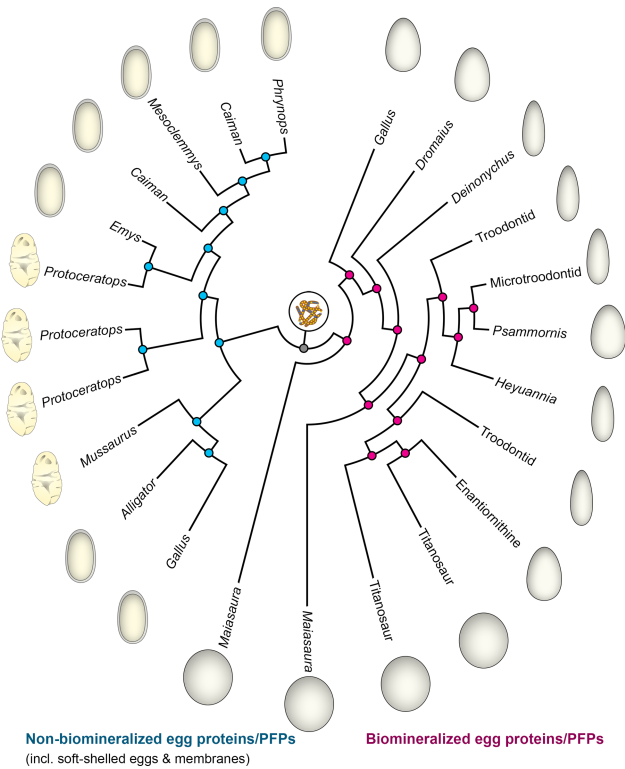
Additional information

Supplementary information is available for this paper at <https://doi.org/10.1038/s41586-020-2412-8>.

Correspondence and requests for materials should be addressed to M.A.N., J.W. or M.F.

Peer review information *Nature* thanks Johan Lindgren and the other, anonymous, reviewer(s) for their contribution to the peer review of this work.

Reprints and permissions information is available at <http://www.nature.com/reprints>.



Extended Data Fig. 1 | Hierarchical cluster analysis of biomineralization signatures preserved in eggshell proteins (extant samples) and their fossilization products (fossil samples). The topology represents a cluster analysis of $n = 24$ selected eggshell protein and PFP bands (Methods). Sampling of both biomineralized proteins (in situ analysis) from hard-shelled eggs and extracted, non-biomineralized membranes from soft and decalcified hard-shelled (*Caiman*, *Alligator*, *Emys*, *Mesoclemmys*, *Phrynosoma* and *Gallus*) eggs avoids phylogenetic attraction of the included fossil samples, and thereby allows eggshell clustering on the basis of the protein and PFP biomineralization signal. Two separate clusters of biomineralized and non-biomineralized eggshell proteins/PFPs are recovered. Pink nodes illustrate biomineralized egg proteins/PFPs, and blue nodes represent non-biomineralized eggshell proteins/PFPs. The egg icons illustrate whether samples represent originally hard or soft eggshell. One spectrum only was used for *Mussaurus*, as there is not much compositional variation across the eggshell (Fig. 1e), whereas all three eggshell spectra were sampled for *Protoceratops*, owing to the differences in composition across the egg section (Fig. 1d). Hard-shelled *Alligator* and turtle eggshells were excluded from this biomineralization analysis, as they do not produce any substantial organic signal with the spectroscopy protocol used (Supplementary Information and ref. 4⁴). Both *Protoceratops* and *Mussaurus* eggshells are nested within the cluster of originally non-biomineralized eggshell proteins/PFPs.

Reporting Summary

Nature Research wishes to improve the reproducibility of the work that we publish. This form provides structure for consistency and transparency in reporting. For further information on Nature Research policies, see [Authors & Referees](#) and the [Editorial Policy Checklist](#).

Statistics

For all statistical analyses, confirm that the following items are present in the figure legend, table legend, main text, or Methods section.

- | n/a | Confirmed |
|-------------------------------------|---|
| <input type="checkbox"/> | <input checked="" type="checkbox"/> The exact sample size (n) for each experimental group/condition, given as a discrete number and unit of measurement |
| <input type="checkbox"/> | <input checked="" type="checkbox"/> A statement on whether measurements were taken from distinct samples or whether the same sample was measured repeatedly |
| <input type="checkbox"/> | <input checked="" type="checkbox"/> The statistical test(s) used AND whether they are one- or two-sided
<i>Only common tests should be described solely by name; describe more complex techniques in the Methods section.</i> |
| <input type="checkbox"/> | <input checked="" type="checkbox"/> A description of all covariates tested |
| <input type="checkbox"/> | <input checked="" type="checkbox"/> A description of any assumptions or corrections, such as tests of normality and adjustment for multiple comparisons |
| <input checked="" type="checkbox"/> | <input type="checkbox"/> A full description of the statistical parameters including central tendency (e.g. means) or other basic estimates (e.g. regression coefficient) AND variation (e.g. standard deviation) or associated estimates of uncertainty (e.g. confidence intervals) |
| <input checked="" type="checkbox"/> | <input type="checkbox"/> For null hypothesis testing, the test statistic (e.g. F , t , r) with confidence intervals, effect sizes, degrees of freedom and P value noted
<i>Give P values as exact values whenever suitable.</i> |
| <input checked="" type="checkbox"/> | <input type="checkbox"/> For Bayesian analysis, information on the choice of priors and Markov chain Monte Carlo settings |
| <input type="checkbox"/> | <input checked="" type="checkbox"/> For hierarchical and complex designs, identification of the appropriate level for tests and full reporting of outcomes |
| <input checked="" type="checkbox"/> | <input type="checkbox"/> Estimates of effect sizes (e.g. Cohen's d , Pearson's r), indicating how they were calculated |

Our web collection on [statistics for biologists](#) contains articles on many of the points above.

Software and code

Policy information about [availability of computer code](#)

Data collection	No customised computer code was used to collect data for this study. All Raman data were collected using the LabSpec 5 software, and all histological sections were imaged using Leica LAS Core Software.
Data analysis	Acquired Raman spectra were standard-processed in SpectraGryph 1.2 spectroscopic software (freeware). Spectral data were stored as taxon-character matrices in Microsoft Excel (Office 365). The DA and Cluster Analysis were run in the PAST 3 software (freeware). An ancestral state reconstruction was run in Mesquite 3.40. Compound figures were created in Photoshop CS5.

For manuscripts utilizing custom algorithms or software that are central to the research but not yet described in published literature, software must be made available to editors/reviewers. We strongly encourage code deposition in a community repository (e.g. GitHub). See the Nature Research [guidelines for submitting code & software](#) for further information.

Data

Policy information about [availability of data](#)

All manuscripts must include a [data availability statement](#). This statement should provide the following information, where applicable:

- Accession codes, unique identifiers, or web links for publicly available datasets
- A list of figures that have associated raw data
- A description of any restrictions on data availability

The authors declare that all relevant Raman spectra and eggshell codings are available within the manuscript and its Supplementary Information. Materials can be made available upon request to the corresponding author.

Field-specific reporting

Please select the one below that is the best fit for your research. If you are not sure, read the appropriate sections before making your selection.

Life sciences Behavioural & social sciences Ecological, evolutionary & environmental sciences

For a reference copy of the document with all sections, see [nature.com/documents/nr-reporting-summary-flat.pdf](https://www.nature.com/documents/nr-reporting-summary-flat.pdf)

Ecological, evolutionary & environmental sciences study design

All studies must disclose on these points even when the disclosure is negative.

Study description	We present mineralogical, organochemical, and ultrastructural evidence for an originally non-biomineralized, soft-shelled nature of exceptionally preserved ornithischian Protoceratops (n=1, spectra with 3 replicates throughout thickness) and basal sauropodomorph Mussaurus eggs (n=1, spectra with 3 replicates throughout thickness). Statistical evaluation (Discriminant Analysis + Hierarchical Cluster Analysis) of in situ organic phase Raman spectra (10 accumulation = technical replicates for each eggshell spectrum) obtained for a representative set of hard- and soft-shelled, fossil and extant diapsid eggshells (total n=24 + n=1 Protoceratops + n=1 Mussaurus), clusters the originally organic, but secondarily phosphatized Protoceratops and the carbonaceous Mussaurus eggshells with soft eggshells. Histology corroborates the organic composition of these two soft-shelled dinosaur eggs, revealing a stratified arrangement resembling soft turtle eggshell. An ancestral state reconstruction (maximum parsimony & maximum likelihood, total n=112 specimens) of composition and ultrastructure compared eggshells from Protoceratops and Mussaurus to those from other archosaurs, and revealed that the first dinosaur egg was soft-shelled. The calcified dinosaur egg evolved at least three times independently throughout the Mesozoic, explaining the bias towards eggshells of highly derived dinosaurs in the fossil record.
Research sample	We used exceptionally preserved ornithischian Protoceratops (n=1, spectra with 3 replicates throughout thickness) and basal sauropodomorph Mussaurus eggs (n=1, spectra with 3 replicates throughout thickness). This material complemented with a total of n=24 hard- and soft-shelled, fossil and extant diapsid eggshells, and eventually contextualised in an Ancestral State Reconstruction covering a total of n=112 specimens (literature-based).
Sampling strategy	No sample size calculation was performed, and Protoceratops and Mussaurus present the only currently known soft dinosaur eggshells. Other hard- and soft-shelled, fossil and extant diapsid eggshells were selected for a representative coverage of the diapsid phylogeny, and the Ancestral State Reconstruction includes all fossil eggshell types published to our knowledge.
Data collection	Mark Norell collected the Protoceratops eggshell specimen, and Diego Pol collected the Mussaurus eggshell specimen. The Protoceratops thin sections were prepared by David Varricchio and Anita Moore-Nall. The Mussaurus thin sections were prepared by Jasmina Wiemann. Jasmina Wiemann designed the Raman spectroscopy protocol, developed the biomineralisation proxy, collected, processed and analysed all Raman and histological data. Matteo Fabbri collected all literature data for the ancestral state reconstruction, and ran the analysis.
Timing and spatial scale	Specimens are housed at the AMNH New York and the Yale Peabody Museum. All data were collected in 2019, at Yale University in New Haven, CT.
Data exclusions	In the cluster analysis shown of hard- and soft-shelled eggs, the organic phase was used to characterise if fossil samples were biomineralised or not. With the requirement of organic spectral signatures, hard-shelled Alligator and turtle eggshells had to be excluded, as they did not produce a significant organic signal with the Raman surface assessment (these are hypercrystalline eggshells). When mapping out Raman signatures of protein fossilisation products, amides, and S-heterocycles across polished egg sections, one of the two soft-shelled dinosaur eggs, the Protoceratops sample, had to be excluded from Raman mapping due to the crumbly nature of the phosphatized organic eggshell. Texture effects resulting from a crumbly surface in a polished section affect Raman signatures, especially in mapping procedures. Signal quality is a pre-determined criterion when analysing fossil organic matter.
Reproducibility	All spectra were acquired with 10 accumulations = technical replicates, and replication of the biomineralisation proxy has been successful!
Randomization	Randomization cannot be applied to this study, because Raman spectra are characteristic for every sample, and can be taxonomically assigned at a glance based on their unique and distinctive taphonomic and compositional signatures. Also, we do not use any statistics that would require randomization. Samples were grouped together based on their identity (eggshell versus sediment), and their degree of biomineralisation (biomineralised versus non-biomineralised). The Principal Component Analysis and Discriminant Analysis shown in the Figs. 3, 4 suggests that samples group based on their organic phase as eggshell or sediment, and as biomineralised or non-biomineralised.
Blinding	Spectral data were analysed 'blinded' for the hierarchical cluster analysis, and sample identity was only revealed in the result of the analysis. Otherwise, blinding did not apply for our study, since Raman spectra of different eggshells contain characteristic spectral features, and are readily identifiable even without associated specimen information.
Did the study involve field work?	<input type="checkbox"/> Yes <input checked="" type="checkbox"/> No

Reporting for specific materials, systems and methods

We require information from authors about some types of materials, experimental systems and methods used in many studies. Here, indicate whether each material, system or method listed is relevant to your study. If you are not sure if a list item applies to your research, read the appropriate section before selecting a response.

Materials & experimental systems

- | n/a | Involvement in the study |
|-------------------------------------|--|
| <input checked="" type="checkbox"/> | <input type="checkbox"/> Antibodies |
| <input checked="" type="checkbox"/> | <input type="checkbox"/> Eukaryotic cell lines |
| <input type="checkbox"/> | <input checked="" type="checkbox"/> Palaeontology |
| <input checked="" type="checkbox"/> | <input type="checkbox"/> Animals and other organisms |
| <input checked="" type="checkbox"/> | <input type="checkbox"/> Human research participants |
| <input checked="" type="checkbox"/> | <input type="checkbox"/> Clinical data |

Methods

- | n/a | Involvement in the study |
|-------------------------------------|---|
| <input checked="" type="checkbox"/> | <input type="checkbox"/> ChIP-seq |
| <input checked="" type="checkbox"/> | <input type="checkbox"/> Flow cytometry |
| <input checked="" type="checkbox"/> | <input type="checkbox"/> MRI-based neuroimaging |

Palaeontology

Specimen provenance

We analyzed a well-preserved ornithischian egg clutch (IGM 100/1021) attributed to Protoceratops from the Ukhaa Tolgod locality (Campanian), Mongolia. Our sample also includes eggs attributed to the basal saurpodomorph Mussaurus (Fig. 1c) from the Laguna Colorada Formation (Late Triassic/Early Jurassic). These were found in the same locality and stratigraphic level as the type material of Mussaurus patagonicus. Several eggs preserve embryonic and juvenile, including elements of the mandible. These elements bear apomorphic features of Mussaurus patagonicus, including a dentary with anterodorsal peg at the symphyseal anterior end

Specimen deposition

The Protoceratops clutch is housed at the AMNH in New York, and the Mussaurus eggshells are housed at the CONICET, Museo Paleontológico Egidio Feruglio, Trelew, Argentina.

Dating methods

No new dates are provided in our study.

- Tick this box to confirm that the raw and calibrated dates are available in the paper or in Supplementary Information.